Journal of Research in Pharmacy

Research Article

www.jrespharm.com

Euphorbia neriifolia L. phytochemical lead compounds discovered using pharmacoinformatic methods as possible SARS CoV-2 main protease inhibitors

Vedanshu MALVIYA[1] *, Mukund TAWAR [1], Prashant BURANGE[2], Ritu BAIRAGI[2], Vaibhav BHADANGE[2], Chaitanya VIKHAR[1]

[1] Department of Pharmaceutics, Faculty of Pharmacy, Sant Gadge Baba Amravati University, Amravati, India.
[2] Department of Pharmaceutical Chemistry, Faculty of Pharmacy Sant Gadge Baba Amravati University, Amravati, India.

*Corresponding Author. E-mail: vedanshumlv56@gmail.com (V.M.); Tel. +91-832-965-2503.

Received: 06 July 2022 / Revised: 25 August 2022 / Accepted: 25 August 2022

ABSTRACT: The corona virus (CoV) family's emerging SARS-CoV-2 strain potentially causes one of the most catastrophic COVID-19 pandemics in mankind. Other than vaccines for preventing SARS-CoV-2 infection, no selective drugs are available to treat the disease caused by the SARS-CoV-2. The main protease (Mpro) of SARS-CoV-2 plays a critical role in viral replication, and inhibiting the protease can hamper the virus's replication and infection process. Thus, we aimed to identify SARS-CoV-2 main protease (Mpro) inhibitors from *Euphorbia neriifolia*. Primarily, a total of 31 compounds were selected through wide literature study and the Indian Medicinal Plants, Phytochemistry and Therapeutics (IMPPAT) server. Current advances in computer-aided drug discovery includes molecular docking, pharmacokinetics, drug properties, toxicity analysis and molecular dynamic (MD) simulation were applied in characterization and identification of possible lead compounds in *E. neriifolia*. The compound's screening through molecular docking resulted in four phytochemicals, viz., CID: 5316673, CID: 102316539, CID: 101257, and CID: 9547213 exhibiting higher binding affinity of -8.461, -7.355, -6.404, and -6.382 kcal/mol, respectively, to the active site of the target Mpro. Subsequently, these four phytochemicals exhibited good pharmacokinetics and drug properties without toxicity. A MD simulation confirmed the binding stability of four phytochemicals to the Mpro. Our study identified four phytochemicals (CID: 5316673, CID: 102316539, CID: 101257, and CID: 9547213) can be developed as treatment option for SARS-CoV-2 disease related complications. Further in vitro and in vivo screening of the anti-SARS-CoV-2 effectiveness of *E. neriifolia*, as well as future clinical studies, are encouraged.

KEYWORDS: SARS-CoV-2; phytochemicals; *euphorbia neriifolia*; molecular protease; molecular docking; pharmacokinetics; drug properties; toxicity; molecular dynamic simulation

1. INTRODUCTION

Corona viruses cause respiratory distress epidemics, including the severe acute respiratory syndrome (SARS) in 2003 [1], with an estimated 10% death rate [2]. Middle East respiratory syndrome (MERS) was first identified in 2012 [3], and severe acute respiratory syndrome-Coronavirus-2 (SARS-CoV-2) was discovered in Wuhan province, China, in 2019 [4-6]. Severe SARS-CoV-2 has been identified as the etiologic mediator of respiratory disfunction disease, a serious condition with increased mortality and illness in global public health issues [7, 8]. An increasing number of whole-genome datasets of the SARS-CoV-2 virus are now being submitted in publicly accessible databases from diverse countries every day [9], and new genome variants give an insight into the uncontrolled infection of SARS-CoV-2 [10]. An important resulting infection caused by COVID-19 has numerous physical signs and symptoms such as fever, chills, cough, shortness of breath, fatigue, but it is also fatal with a 6% death frequency, resulting from massive alveolar damage and progressive respirational failure [11, 12]. Almost two years later, SARS-CoV-2 is still recognized as the causal mediator of the severe acute respiratory syndrome that generates a worldwide health risk. Currently, researchers have focused on the phytochemicals of medicinal plants for effective compounds against SARS-CoV-2 [13, 14]. The phytochemicals' antiviral function against several viral diseases has previously been established in the field of infectious diseases research [15, 16]. Therefore, secondary compound isolation and

How to cite this article: Malviya V, Tawar M, Burange P, Bairagi R, Bhadange V, Vikhar C. *Euphorbia neriifolia* L. phytochemical lead compounds discovered using pharmacoinformatic methods as possible SARS CoV-2 main protease inhibitors. J Res Pharm. 2023; 27(1): 157-172.

ISSN: 2630-6344

http://dx.doi.org/10.29228/jrp.300

investigation of numerous pharmacological activities have been recognized as a vital aspect of drug discovery [17].

SARS CoV-2 is a family member of Coronaviridae and comprises a positive-sense single-stranded RNA genome of about 30 kb which translates four structural proteins and sixteen nonstructural proteins [2]. SARS-CoV-2 enters the host cell primarily through the spike (S) protein, a structural protein of SARS-CoV-2 that eventually binds to the angiotensin-converting enzyme 2 (ACE2) receptor [2, 18]. One of the coronaviral non-structural proteins, the main protease (Mpro or 3CLpro), which is responsible for the viral duplication, is associated with producing twelve non-structural proteins (Nsp4-Nsp16) and the viral polyproteins [19]. To promote a massive and terrible infection in the respiratory organ, vast replicas of the transmittable virus must be replicated, and the RNA-dependent RNA polymerase (RdRp, Nsp12) and helicase (Nsp13) [20] that cleaves from the main protease are responsible for upholding this machinery. Therefore, the inhibition of Mpro, the main protease, can be the superlative prevention strategy of the virus that halts replication and establishes one of the potential anti-coronaviral treatments [21].

E. neriifolia L. belongs to the family Euphorbiaceae and is a barbed and spiny herb available in Bangladesh [22-25]. Locally, it is known as "Dudhsar or Mansasij." For many years, the tribal people of Varendra, a region of North Bengal in Bangladesh and West Bengal in India, have used the leaf juice of *Euphorbia neriifolia* as an antidote for colds, coughs, fevers, asthma, pneumonia, and bronchitis [25]. It is also native to Southeast Asia and is currently cultivated in southern Taiwan, where it was previously studied as an antiviral medicinal plant against the SARS coronavirus [26]. The antiviral activity of the separated triterpenoids from plant extract was studied, which was found in the ethanolic extract of *E. neriifolia* leaves and revealed a structure-activity connection against the human coronavirus (HCoV) [27]. The potential anti-viral action of *E. neriifolia* against human SARS coronavirus with the 23 compounds, including 22 triterpenoids and one flavonoid glycoside, which were isolated [28], indicates an exciting prospect in discovering a novel drug against the current mischief-maker, SARS CoV-2. In Bangladesh, during the COVID pandemic, it was an issue generating a significant amount of coverage and discussion in all the renowned news journals that the leaf juice of *E. neriifolia* was used locally as a treatment strategy and found an auspicious review from those COVID-infected people who used this plant's leaf juice as a traditional medicinal plant.

In our current study, we use computational approaches for designing potential drugs by using the plant isolated compounds of *E. neriifolia* L. targeting the Mpro protease based on its previous and current studies reports, which indicate a good sign for designing a promising drug against SARS CoV-2. Current advances in computer-aided drug discovery have dispelled all the blockades to identifying compounds, potential drug targets, and screening or repurposing approved drugs against a specific target. Computational drug design approaches comprise compound identification, computer-generated screening, molecular docking, and molecular dynamics (MD), which is the most widely used tactic to design and evaluate drugs and biologically dynamic molecules against a definite target [29, 30]. That's why the drug design against SARS CoV-2 Mpro protease applied computer-aided drug design (CADD) methods including molecular docking, MD simulation, and validation approaches to recognize and screen phytochemical compounds of *E. neriifolia* L. plant to identify elegant drug candidates.

2. RESULTS

2.1. Extra precision (XP) molecular docking simulations showed good binding affinity between the target protein and ligands.

Molecular docking could predict both the binding affinity between ligand and protein and the structure of the protein-ligand complex, which is useful information for lead optimization. Thus, a molecular docking study was carried out for the determination of the best intramolecular binding affinities of the Mpro of the SARS-CoV-2 (PDB ID: 6W63) structure and 31 phytochemical-ligands with one control ligand (Table 1) by using the Schrodinger suite version 2020-3. The binding scores showed a lower distributed value of -3.763kcal/mol and the highest distributed value of -8.461kcal/mol. In this study, X77 showed a binding energy of -6.239 kcal/mol rather than the other top four phytochemicals: CID: 9547213, CID: 101257, CID: 102316539, and CID: 5316673 showed binding energies of 6.382, -6.404, -7.355, and -8.461 kcal/mol, respectively. It has been reported that X77 is an inhibitor of Mpro of SARS-CoV-2 (PDB ID: 6W63). Based on the binding score, among 31 phytochemicals, these 4 phytochemicals exhibited better binding affinities compared to the control ligand (X77). These four compounds were considered for further evaluation in this study.

Table 1. The selected four phytochemicals and targeted MproofSARS-CoV-2 binding interactions were simulated during molecular docking simulations.

Compounds name	Compounds CID	Canonical SMILES	Docking score	H-bond	Other interactions
Afzelin	CID: 5316673	CC1C(C(C(C(O1)OC2=C(OC3=CC(=CC(=C3C2=O)O)O)C4=CC=C(C=C4)O)O)O)O	-8.461	CYS44, THR190, GLU166, ASN142	HIE41, TYR54, PRO52, MET49, ASP187, ARG188, GLN189, ALA191, GLN192, PRO168, GLU166, MET165, HIE163, CYS145, GLY143
Neriifolione	CID: 102316539	CC(C)C(CCC(=C)C1CCC2(C1(CCC34C2CCC5C3(C4)CCC(=O)C5(C)C)C)C)O	-7.355	THR190, GLN192	THR25, THR24, MET49, SER46, THR45, CYS44, VAL42, HIE41, VAL186, CYS145, ASP187, ARG188, GLN189, ALA191, PRO168, LEU167, GLU166, MET165, HIE164
Tirucallol	CID: 101257	CC(CCC=C(C)C)C1CCC2(C1(CCC3=C2CCC4C3(CCC(C4(C)C)O)C)C)C	-6.404	THR26	HIE41, VAL42, CYS44, TYR54, PRO52, MET49, VAL186, ASP187, ARG188, GLN189, THR190, ALA191, GLN192, ASN142, GLY143, SER144, CYS145, THR25, LEU27, HIE164, MET165, GLU166, LEU167, PRO168
24-methylene-cycloartanol	CID: 9547213	CC(C)C(=C)CCC(C)C1CCC2(C1(CCC34C2CCC5C3(C4)CCC(C5(C)C)O)C)C	-6.382	THR26	HIE41, VAL42, CYS44, THR45, SER46, MET49, PRO52, TYR54, GLN192, THR190, PRO168, LEU167, GLN189, GLU166, ARG188, MET165, ASP187, VAL186, HIE164, PHE181, CYS145, SER144, GLY143, ASN142, LEU27, THR25, THR24
Control ligand (X77 or N-(4-tert-butylphenyl)-N-[(1R)-2-(cyclohexylamino)-2-oxo-1-(pyridin-3-yl)ethyl]-1H-imidazole-4-carboxamide)	CID-145998279	CC(C)(C)C1=CC=C(C=C1)N(C(C2=CN=CC=C2)C(=O)NC3CCCCC3)C(=O)C4=CN=CN4	-6.239	GLU166, HIE163, GLY143	THR25, THR26, LEU27, MET49, PRO52, TYR54, THR190, GLN189, ARG188, ASP187, GLN192, PRO168, LEU167, GLU166, MET165, HIE163, HIE172, PHE172, PHE140, LEU141, ASN142, GLY143, SER144, CYS145, HIE41, VAL42, CYS44

2.2. Interpretations of the protein-ligands binding interaction

The four best-scoring ligands were selected for binding analysis of the interaction formed with the desired protein, and the interacting bond type with residues is visualized by using the Maestro (v12.5). As shown in Table 1 and Figure 1, several types of non-bonded interactions, such as conventional hydrogen bonds, hydrophilic and hydrophobic bonds, electrostatic bonds, and polar bonds, have been found to form the interaction with the Mpro of SARS-CoV-2. In CID: 5316673, four hydrogen bonds have been found to form with CYS44, THR190, GLU166, and ASN142, and other interacting bonds have been observed at the position of the residues of HIE41, TYR54, PRO52, MET49, ASP187, ARG188, GLN189, ALA191, GLN192, PRO168, GLU166, MET165, HIE163, CYS145, and GLY143 (Figure 1A). Two H-bonds (THR190, GLN192) and other bonds (THR25, THR24, MET49, SER46, THR45, CYS44, VAL42, HIE41, VAL186, CYS145, ASP187, ARG188, GLN189, ALA191, PRO168, LEU167, GLU166, MET165, HIE164) have been found in the second-highest binding scored compound, CID: 102316539 (Figure 1B). One hydrogen bond was observed at the THR26 amino acid residue position in CID: 101257 (Figure 1C) and CID: 9547213 (Figure 1D) from the interaction between protein and ligand. The interactions in the control compound (X77) have formed three H-bonds (GLU166, HIE163, and GLY143), which is higher than the interactions formed by H-bonds in three selected compounds (CID: 102316539, CID: 101257, and CID: 9547213) and lower than the interactions formed by H-bonds in CID: 5316673. In the selected compounds, THR 190 was the common interacting atom in the first two ligands (CID: 5316673 and CID: 102316539) and THR26 for the last two ligands (CID: 101257 and CID: 9547213), but the residues were not present in the control compound (X77).

2.3. The selected four phytochemicals exhibited pharmacokinetics, and drug-able and toxicity properties to be the possible drug candidate

The bioavailability of the drug is greatly affected by the pharmacokinetic properties (GI absorption and BBB permeate). Therefore, GI absorption and BBB permeant were determined. In our results, we found that although the selected best phytochemicals have lower GI absorption ability, they are not BBB permeant, an indication that they are non-CNS target. Effective drug development involves a comprehensive evaluation of rationalization of drug properties and toxicity. These properties greatly influence the pharmacokinetics of the drug candidates. Thus, in this study, Swiss ADME server was used to quantify these properties (Table 2) for the best four (based on docking score) phytochemicals. These phytochemicals exhibited acceptable ranges of MW (<500 g/mol), HBA (≤10), HBD (≤5), and RB (3 to 5). All the four phytochemicals (CID: 5316673, CID: 102316539, CID: 101257, and CID: 9547213) showed only one RO5 violation. The synthetic feasibility of a drug candidate is an important factor, for this reason, computational and medicinal chemists consider this as a basic objective in the early drug development stage. The compounds with a synthetic accessibility score (SA score) ≥6 is challenging to synthesize, and SA score ≤6 is easy to synthesize. All four phytochemicals showed favorable synthetic accessibility (SA score ≤6) with the expected desired properties. Toxicity prediction is essential in the current drug discovery process for assessing a compound's adverse effects on humans, animals, and the environment. Liver toxicity is one of the most critical aspects of the medication development process. The hepatotoxicity test revealed that all four phytochemicals were not hepatotoxic. Acute oral toxicity is an essential endpoint in medicinal research and environmental hazard management. However, the experiments are tedious to conduct; therefore, in silico approaches have been developed as a replacement. The United States Environmental Protection Agency (EPA) has classified toxicity grounded on LD50, and we found that all four phytochemicals are not acutely toxic. An obstacle to medicinal agents is carcinogenicity, which becomes severe when linked with mutagenicity. All four phytochemicals were found to be non-mutagenic and non-carcinogenic.

2.4. Molecular dynamics (MD) simulations

In our study, to determine the physical movement of atoms and macromolecules, the top four phytochemicals, along with one reference structure (apo), were performed with a reference time of 100 ns in MD simulation, and the trajectory output was evaluated for the analysis of the results. The trajectory was analyzed and illustrates the pose based on RMSD, RMSF, rGyr, SASA, and protein-ligand contact.

Journal of Research in Pharmacy
Research Article

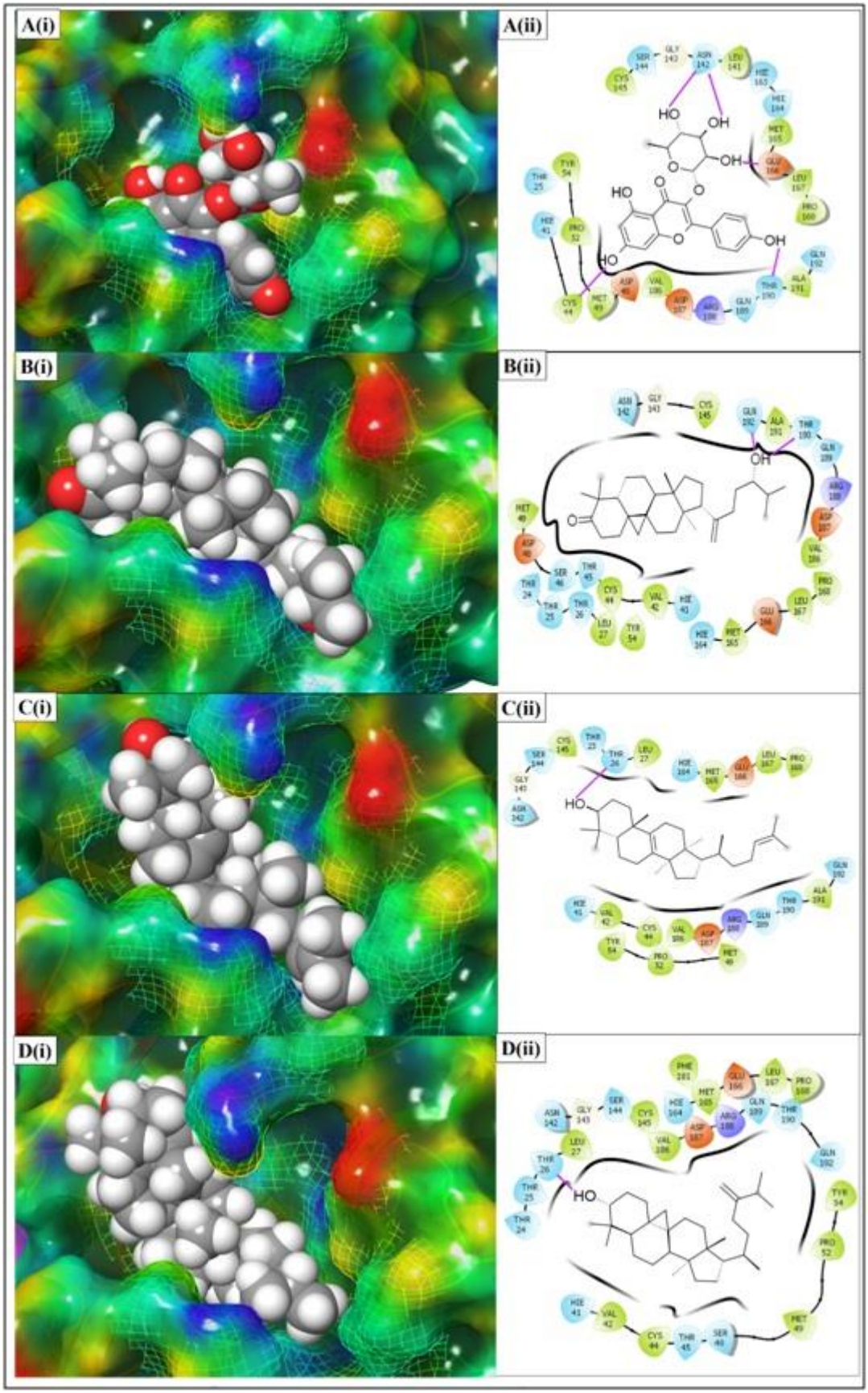

Figure 1. Molecular docking interaction between the SARS-CoV-2 Mpro and selected four compounds in 3D left and 2D right. Depicting the phytochemicals, A (i, ii) CID:5316673, B (i, ii) CID:102316539, C(i, ii) CID:101257,and D(i, ii) CID:9547213in the active pocket of Mpro.

http://dx.doi.org/10.29228/jrp.300
J Res Pharm 2023; 27(1): 157-172

Table 2. Pharmacokinetics (ADME), drug properties (physicochemical, lipophilicity, water-solubility, drug-likeness, and medicinal chemistry) and toxicity of selected four compounds.

CID Number			**CID: 5316673**	**CID: 102316539**	**CID:101257**	**CID: 9547213**
Pharmacokinetics		GI absorption	low	low	low	low
		BBB permeant	no	no	no	no
Drug- Properties	Physicochemical properties	MW (g/mol)	432.38	440.7	426.72	440.74
		Heavy atoms	31	32	31	32
		Aromatic heavy atoms	16	0	0	0
		Rotatable bonds	3	5	4	5
		H-bond acceptors	10	2	1	1
		H-bond donors	6	1	1	1
	Lipophilicity	Log Po/w(MLOGP)	-1.34	5.89	6.82	7.12
	Water Solubility	Log S (ESOL)	-3.47	-7.53	-7.83	-8.74
	Drug likeness	Lipinski's rule of 5 (RO5)violation	Yes; 1 violation (NH or OH>5)	Yes; 1 violation (MLOGP>4.15)	Yes; 1 violation (MLOGP>4.15)	Yes; 1 violation (MLOGP>4.15)
	Medicinal Chemistry	Synthetic accessibility	5.25	6.12	6.07	6.36
Mutagenicity and Toxicity		Carcinogenicity (probability)	Inactive (0.50)	Inactive (0.62)	Inactive (0.55)	Inactive (0.61)
		Mutagenicity (probability)	Inactive (0.71)	Inactive (0.97)	Inactive (0.94)	Inactive (0.74)
		Hepatotoxicity (probability)	Inactive (0.73)	Inactive (0.69)	Inactive (0.58)	Inactive (0.92)
		Cytotoxicity (probability)	Inactive (0.93)	Inactive (0.93)	Inactive (0.96)	Inactive (0.85)
		LD50 (mg/kg)	5000	1000	2000	5000
		Toxicity class	5	4	4	5

2.5. RMSD analysis

In MD simulation, the root-mean-square deviation (RMSD) is considered the root-mean-square error (RMSE) that helps to determine whether the simulation has equilibrated or not by calculating the mean value change by dislocation of atoms from a particular frame compared to a reference frame. With a range of 1–3 Å, the average change in RMSD of the protein-ligand complex is perfectly acceptable. If the RMSD value is greater than 1–3 Å, the protein structure has undergone a significant conformational shift. If the dislocation of Apo atoms is equivalently equal to the selected ligand, the ligand is considered favorable. As shown in Figure 2, selected protein-ligand complexes CID: 5316673 (orange), CID: 102316539 (grey), CID: 101257 (yellow) and CID: 9547213 (dark blue) are compared with two reference structures, Apo-form (lite blue), and the control ligand CID-145998279 (green). In the CID:5316673 (orange), the highest RMSD was 2.096 Å and the lowest RMSD was 0.822 Å, in CID-102316539 (grey), the highest RMSD was 2.335 Å and the lowest RMSD was 0.876, in CID: 101257 (yellow), the highest RMSD was 2.542 Å and the lowest RMSD was 1.121 Å and in CID: 9547213 (dark blue), the highest RMSD was 2.127Å and the lowest RMSD was 0.966 Å compared with apo (lite blue) and control ligand CID-145998279 (green), where the highest and lowest

RMSD were 2.193 Å, 0.958 Å, and 2.184 Å, 0.899 Å, respectively. The difference between the highest and lowest RMSD in CID-5316673 (orange) was nearly the same as Apo and has been shown to differ from the control ligand. Moreover, the lower average fluctuation was 1.326 Å as shown in CID-5316673 (orange), which was better than both apo and control. All the compound's RMSD values are confined to 1-3 Å. So, both the four selected compounds, CID-5316673 (orange), CID-102316539 (grey), CID: 101257 (yellow) and CID: 9547213 (dark blue) show decent stability in comparison to the Apo fluctuation distance, but CID-5316673 (orange) is more promising.

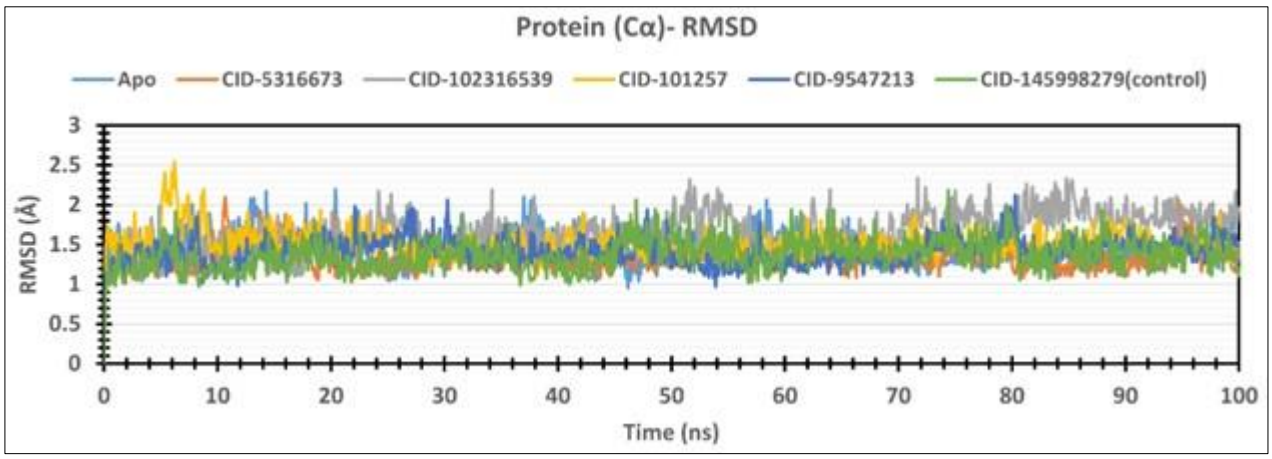

Figure 2. RMSD values were extracted for alpha carbon (Cα) atoms (lite blue curves) of SARS-CoV-2 Mpro apo protein, control compounds (green curves) of CID-145998279, and phytochemicals of CID-5316673 (orange curves), CID-102316539 (grey curves), CID-101257 (yellow curves), and CID-9547213 (dark blue) from the MD simulation.

2.6. RMSF analysis

The root mean square fluctuation (RMSF) is examined to understand the local conformational change of a protein that calculates the displacement of specific amino acid residues. RMSF is a numerical measurement process that is needed for characterization and determining the macromolecules' heterogenicity and steady-state. As shown in Figure 3, the highest peaks of fluctuation were observed in Asp48, Pro168, Asn221, and Leu227 residual positions where all the compounds' amino acid residues show minimal fluctuation of around 1Å and maximum fluctuation was found at 2.481Å in Asp 48 residue for the complex of CID-102316539 (grey).The average fluctuation was 0.912, 0.871, 0.914, 0.842, 0.918, and 0.823 Å for apo (lite blue), CID-5316673 (orange), CID-102316539 (grey), CID-101257 (yellow), CID-9547213 (dark blue), and control ligand CID-145998279 (green), respectively. All the selected compounds' fluctuation was optimal compared with apo and control compounds, indicating the protein complex had shown the most flexibility without changing the macromolecular structure.

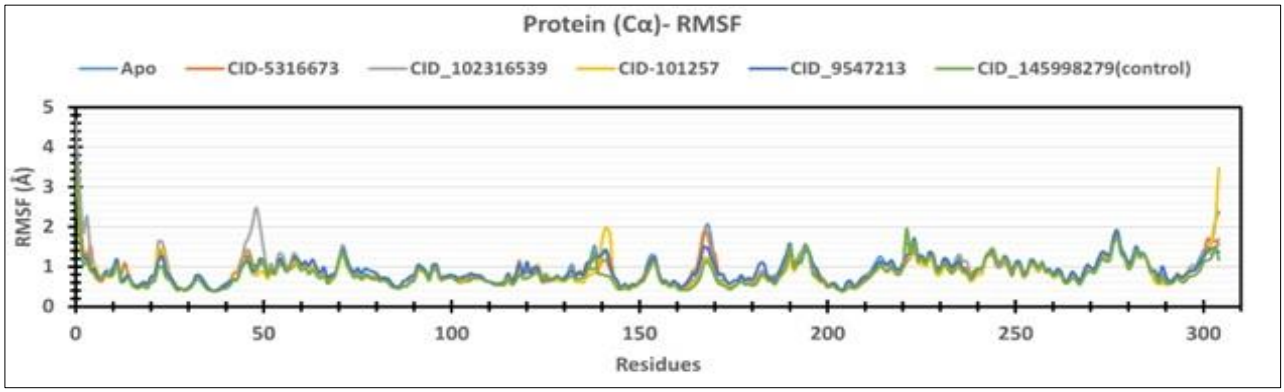

Figure 3. The RMSF values of SARS-CoV-2 Mpro were extracted from the protein Cα atoms of the protein-ligand docked complexes. The RMSF of the native Mpro apo protein (lite blue curves), and the selected four phytochemicals are CID-5316673 (orange curves), CID-102316539 (grey curves), CID: 101257 (yellow curves), CID-9547213 (dark blue curves), and the control compound CID-145998279 (green curves) from the MD simulation.

2.7. The radius of gyration (rGyr) analysis

The radius of gyration (rGyr) analysis in Figure 4 reveals that after interaction with the ligands, the receptor's active site does not exhibit any notable deformation. The root means a square radial distance from the center of mass of the target protein to both of its terminal mobility and rigidity measurement processes, which is known as the radius of gyration (rGyr). Therefore, the average alteration of the protein-ligand complex compactness, which is determined by the macromolecule's structural activity, was analyzed. In our 100 ns simulation, the average rGyr was found to be 4.11, 4.65, 4.51, 4.71, and 4.15 for the phytochemicals of CID-5316673 (lite blue), CID-102316539 (orange), CID-101257 (grey), and CID-9547213 (yellow) compared with control ligand CID-145998279 (dark blue), respectively, which indicates that the active site of the receptor does not undergo any major conformational changes after binding with the ligands.

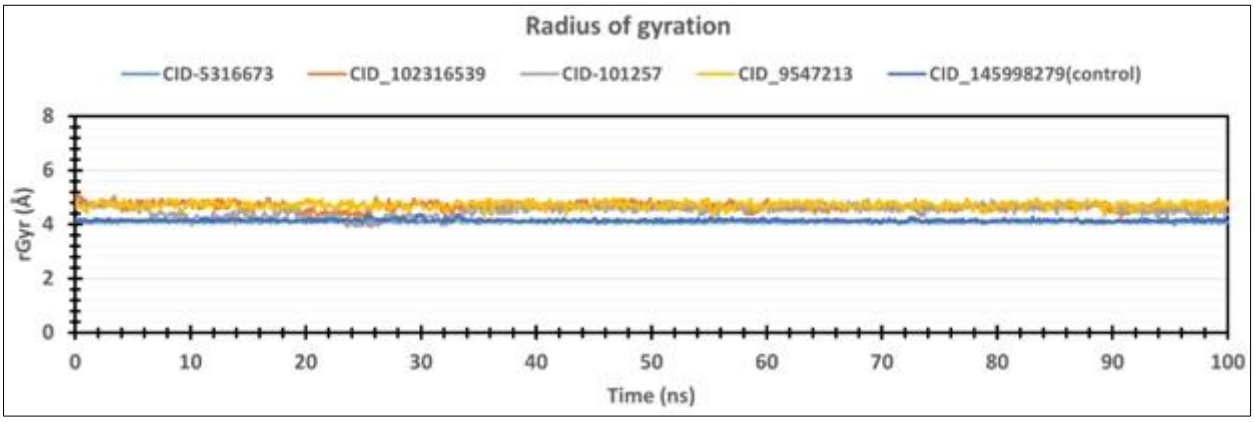

Figure 4. The radius of gyration (rGyr) values is extracted from the complex structure of the protein-ligand complex. The rGyr value was represented for four phytochemicals of CID-5316673 (lite blue curves), CID-102316539 (orange curves), CID-101257 (grey curves), and CID-9547213 (yellow curves), as well as the control ligand, CID-145998279 (dark blue curves).

2.8. Solvent accessible surface area (SASA) analysis

The protein and protein complex's stability and hydrophilic or hydrophobic solvent-like behavior are characterized by solvent-accessible surface area (SASA). The receptor surface amino acid interacts with ligands at the active site to ensure the solvent-like behavior of the protein-ligand complex. Therefore, the SASA value of protein in complex with the phytochemicals of CID-5316673 (faint blue), CID-102316539 (orange), CID-101257 (grey), and CID-9547213 (yellow), compared with the control ligand CID-145998279 (dark blue), was calculated and presented in Figure 5.

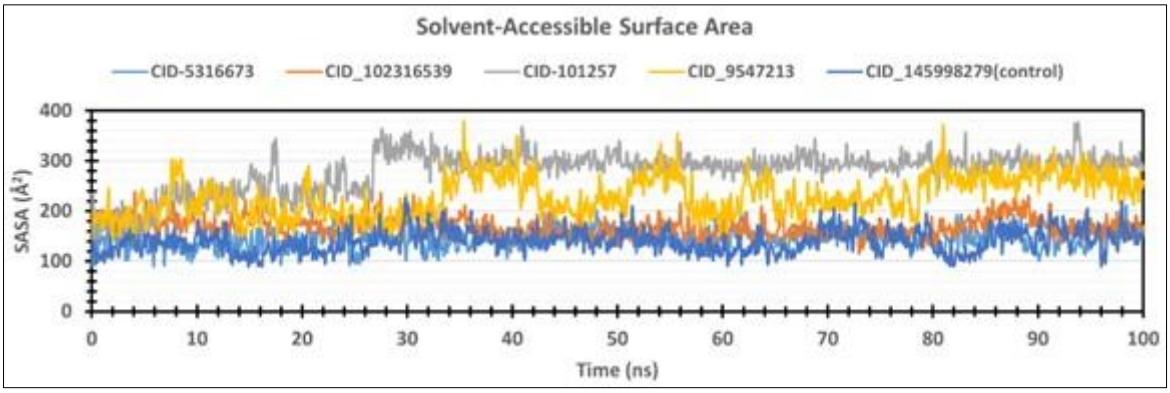

Figure 5. The solvent accessible surface area (SASA) of the selected protein-ligand complexes was calculated during the 100 ns MD simulation. The SASA value was represented for four phytochemicals of CID-5316673 (lite blue curves), CID-102316539 (orange curves), CID-101257 (grey curves), and CID-9547213 (yellow curves), as well as the control ligand, CID-145998279 (dark blue curves).

2.9. Protein-ligand contact analysis

The targeted protein complex with the selected biological compounds CID-5316673, CID-102316539, CID-101257, CID-9547213 and control ligand CID-145998279 intra-molecular interactions have been analyzed by different multiple types of bonding interactions like hydrogen bonds, hydrophobic bonds, ionic and water bridges using the simulation interaction diagram (SID) during the 100ns MD simulation shown in Figure 6. Different types of binding interactions play an important role in the ligand-binding of a protein complex. These four amino acids MET49, MET165, GLU166, and PRO168 positions have been shown to have common binding interactions in control and four selected ligands, which is necessary for the desired drug's stable binding with the target protein. In four common binding positions, all the selected compounds produce not only hydrogen bonds but also multiple types of bonds that were found to form multiple binding interactions at the same residues.

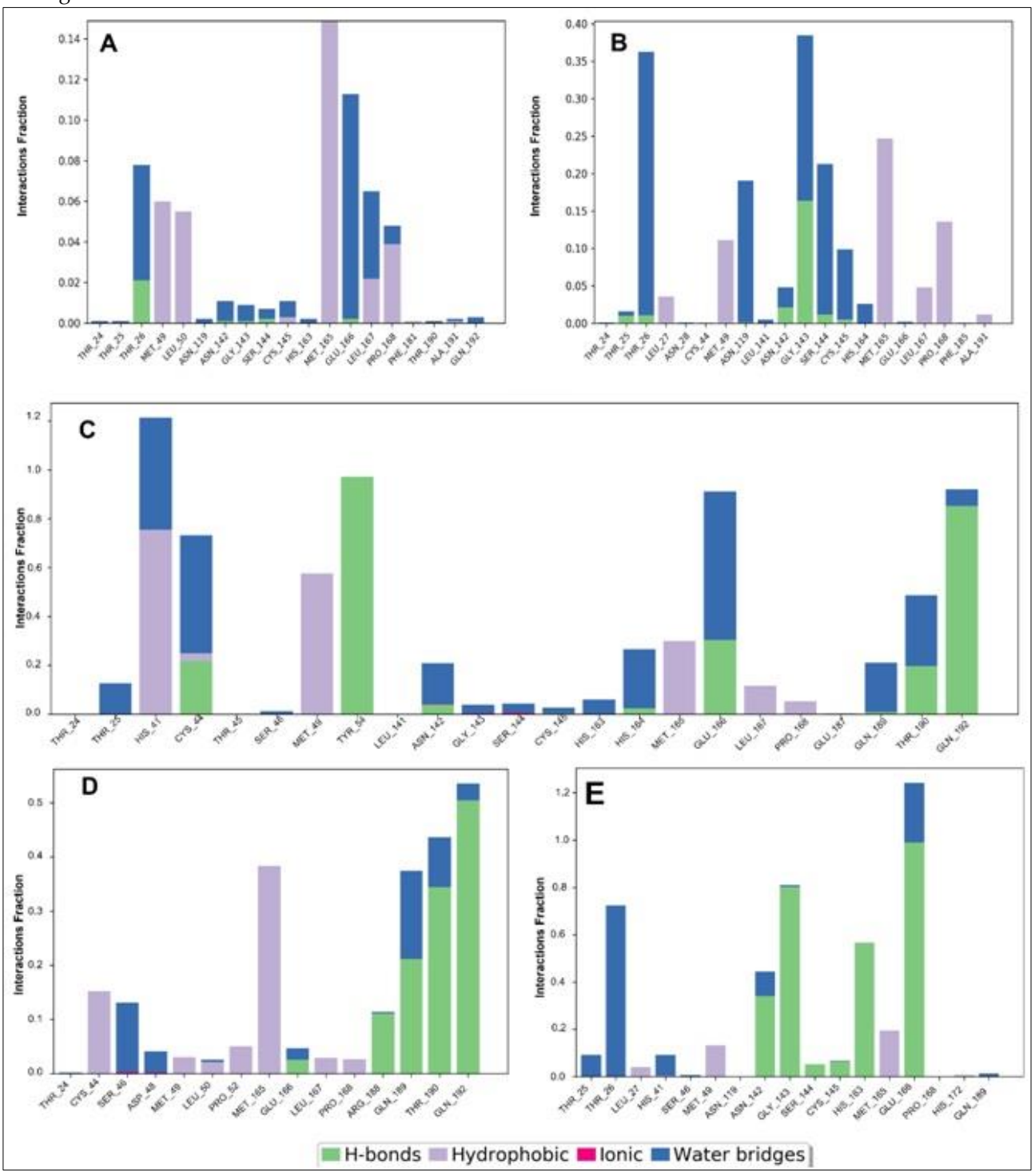

Figure 6. The different types of bonding that occurred along the protein-ligand contact during the 100 ns MD simulations.(A) CID-101257, (B) CID-9547213, (C) CID-5316673, (D) CID-102316539, and (E) CID-145998279).

3. DISCUSSION

SARS-CoV-2, the causal mediator of dreadful respiratory diseases, created havoc, and the incidence of suspected re-infections over time is still uncontrolled [45, 46]. Different new variant emerged recently, causing a deteriorated situation by infecting the huge human population and severely impeding public health care [47-49]. The worldwide terrible situation gives an insight into discovering novel drugs and diverse medication approaches that are trying to be established as ideal treatments for infected patients. Phytochemicals have been obtained from plants for thousands of years; they've been proven to be effective pharmaceutically active ingredients, and they're a key player in infectious disease treatment tactics [50, 51]. The public health sector is desperate for a novel therapeutic agent to end COVID-19's infectious disease, and researchers from around the world have been scouring medicinal plants for potential phytochemicals that are protective against several enzymes and other proteins involved in SARS-CoV-2 replication and transcription[52]. The herb E. neriifolia L. was previously researched as a viral activity inhibitor via an unknown mechanism and was traditionally used for coughs and colds, bronchitis, fevers, and chronic respiratory problems, but its activity as a SARS-CoV-2 pharmaceutical option is still unknown[53]. As a result, the study's goal is to determine the potential of Euphorbia neriifolia L. as a promising natural Mpro inhibitor, followed by computational ways to overcome the existing graving conditions caused by SARS-CoV-2.

In our work, we found promising therapeutic options against SARS-CoV-2 by focusing on the virus's Mpro[54]. Initially, the 18 phytochemicals of the Euphorbia neriifolia plant were found using public data from a research study and 13 phytochemicals from a curated database called IMPPAT[55-58].Following that, the total of 31 compounds found were screened using molecular docking, and four compounds were chosen when compared to a control ligand. Among 31 phytochemicals, these phytochemicals (CID: 5316673, CID: 102316539, CID: 101257, & CID: 9547213) have a higher binding affinity with Mpro than the control ligand. The phytochemicals incorporated the SARS-CoV-2 Mpro's active pockets, from which the first two compounds (CID: 5316673, CID: 102316539) frequently interacted with THR190 residues and the last two compounds (CID: 101257 & CID: 9547213) interacted with THR26 residues.

The pharmacokinetics related to ADME fundamentally dictate the security and adequacy of medication since the most widely recognized reason for drug disappointment in clinical trials is weak ADME [59]. Accordingly, the pharmacokinetic boundaries should be upgraded through the medication configuration stage to succeed the standard clinical trials, which should have been a promising medication competitor. Therefore, we investigated the pharmacokinetics in the context of GI absorption and BBB permeant and found that the four best phytochemicals selected based on docking score although have lower GI absorption ability but are not permeable to the CNS, indicating that they are not CNS targets. One of the essential functions of the BBB is to protect the CNS against xenobiotics [60-62]. Our selected phytochemicals are pointing towards other parts of the body other than the CNS and keeping away from psychotropic effects. Successful drug development entails an accurate evaluation and rationalization of drug-able properties, including physicochemical (MW, aromatic heavy atoms, RB, HBA, and HBD), lipophilicity, water-solubility, and drug-likeness (RO5), which are all associated with the bioavailability of drug molecules [63, 64]. The ideal molecular weight of a drug is ≤500 g/mol and the permeability of a drug candidate can be increased as the molecular weight decreases, and each of our selected four phytochemicals has an ideal molecular weight (<500 g/mol)[65].Our analysis of selected phytochemicals showed that they all showed optimal drug-able properties. Synthetic accessibility score (SA score) is designed to estimate the feasibility of the synthesis of drug-like molecules [66]. The compounds with SA score ≥6 are challenging to synthesize, and SA score ≤6 are easy to synthesize. All four phytochemicals are showed synthetic accessibility with the expected desired value (SA score ≤6). Toxicity is a condition in which a substance is poisonous and can harm an organism [67]. Its assessment is a significant stage in the cutting-edge drug designing process that assists in determining the dose or concentration of administration. The unexpected side effects of a particular drug compound can also be avoided by estimating the level of toxicity with respect to the amount of dose. Furthermore, this early assessment can save time and money and reduce the risk of failure at the penultimate time. Therefore, the toxicity of phytochemicals was assessed through the mutagenicity, carcinogenicity, hepatotoxicity, and Rat oral acute toxicity in silico [68]. Medicinal agent carcinogenicity is a

critical issue, and mutagenicity is linked to carcinogenicity. Liver toxicity is one of the most critical aspects of the medication development process. In silico models grounded on the molecular organization can assist emphasize lab investigations, preclinical investigations, and clinical trials, which can help to assess hepatotoxicity. Our in-silico study resulted from those 4 phytochemicals that are not toxic for hepatocytes. In pharmaceutical research, acute oral toxicity is a serious issue [69]. Since tests are dreary for conduct, in silico approaches have been formed as a substitution. The United States Environmental Protection Agency (EPA) has created toxicity classes grounded on LD50[70, 71]and 4 selected phytochemicals were determined to be not acutely toxic as their LD50 value are ≥1000 mg/kg. The idea of drug-likeness has been widely attributed to filtering out compounds [72]with undesired qualities. Lipinski suggested the drug-likeness (Rule of Five, RO5), which stipulates the four basic physicochemical properties are MW (<500 g/mol), HBA (≤10), HBD (≤5), and MlogP (>4.15).Thus, the drug-likeness of the identified phytochemicals was also validated using the RO5, which is all correlated with higher bioavailability of drug molecules. In our study, we found that each of the four phytochemicals that showed the best binding affinity with the target protein had one RO5 violation in the context of HBD with CID: 5316673, and MlogP with CID: 102316539, CID: 101257, CID: 101257, and CID: 9547213.Similarly, there is evidence of some FDA-approved drugs with one violation in the hydrogen bond donor parameter that have good interaction with target molecules [72, 73].

The stability of a protein in a compound with ligands is investigated using molecular dynamics simulations [74]. In a regulated environment, such as the human body, it can also determine the stability and stiffness of protein-ligand complexes [75, 76]. The RMSD values of complex systems show the compounds' greatest stability, whereas the measure of the RMSF value means fluctuation, which is used to estimate the compactness of the protein-ligand complex [77]. The RMSD of the system was calculated using the C atoms of the protein-ligand complexes, confirming the protein's minimal variation. The RMSF value was used to determine the fluctuation of the protein, which also confirmed the minimal fluctuation of the complex system, indicating the stability of the chemicals to the target protein. Forrgyr computed, the center of mass from the protein C and N terminals examines the protein structure's stability and provides a broader understanding of protein folding features [77].The lower the rGyr value, the higher the compactness, and the greater the value, the more the compounds are disassociated from the protein, and all four phytochemicals have a higher rGyr value [78]. The higher the SASA number, the less stable the structure is, whereas the lower the value, the tighter the complex of water molecules and amino acid residues is [79].The investigation revealed the four drugs' optimal rGyr and SASA values. The findings of the evaluation of four compounds based on different factors were mixed, so the phytochemicals should be chosen for further testing using various wet lab-based experimental procedures.

4. CONCLUSION

Drug design appears to be a very popular, effective, and external strategy to find inhibitory drugs for a certain target protein. In this study, we identified novel natural Mpro inhibitors using a computer-aided drug design (CADD) approach that includes compound selection, drug-like properties analysis, molecular docking, and MD simulation approaches. Our computational research identified the potential of four lead phytochemicals of CID: 5316673 (Afzelin), CID: 102316539 (Neriifolione), CID: 101257 (Tirucallol), and CID: 9547213 (24-methylene-cycloartanol) to inhibit the virulence activity of Mpro and interact through restricting SARS CoV-2 from multiplying inside the human host organism.

5. MATERIALS AND METHODS

5.1. Protein preparation

The three-dimensional X-ray crystallographic structure of the Mpro enzyme of SARS-CoV-2 (PDB: 6W63) was revised from the RCSB protein data bank (PDB) (https://www.rcsb.org/)[31]. The atomic structure of the protein was resolved by the X-ray diffraction method with 2.10 Å resolution and contained 306 amino acids at length. At first, the protein preparation wizard of the Schrodinger suite version 2020-3 was subjected to the preparation of the protein by assigning bond orders, creating zero-order bonds to metals and disulfide bonds to fill the missing side chains, and removing water from the protein [32]. Finally, the Optimized Potential for Liquid Simulations (OPLS-3e) force field was utilized for refinement and energy minimization of the protein crystal structure [33].

5.2. Retrieval and preparation of phytochemical ligands

Thirty-one phytochemicals (Supplementary Table 1) were identified for E. neriifolia through extensive literature study [28] and the IMPPAT server (https://cb.imsc.res.in/imppat/home). 3D structure of 31 phytochemicals were retrieved from the PubChem database [34] (https://pubchem.ncbi.nlm.nih.gov/) and the IMPPAT server. Afterward, the Ligprep wizard of the Maestro Schrodinger suite was utilized for processing and preparation of the bioactive ligand molecules [33]. The 3D structure of the ligand high-energy ionization states was minimized and generated by using Epik version v5.3 at pH 7.0 ± 2. Furthermore, the OPLS3e force field was applied, which generated 236 possible stereoisomers by determining possible chiral centers on each molecule and was employed for another minimization.

5.3. Binding site identification and receptor grid generation

The binding site (BS) of the ligand to the target protein molecule was selected by considering the binding site of the reference ligand,N-(4-tert-butylphenyl)-N-[(1R)-2-(cyclohexylamino)-2-oxo-1-(pyridin-3-yl) ethyl]-1H-imidazole-4-carboxamide (X77) to a region where some specific amino acid residues of Mpro allow the protein to bind with the ligand, X77 [35].Co-crystallized reference ligand (X77) attaching residues at the selected position of Mpro was selected by generating grid box as the binding site of test ligand[36]. The grid was adapted to grid version 81012 and the grid ranges X =-20.595, Y = 18.084, Z =-26.996, resulting in a cubic box encircling the receptor protein's binding site. The grid box was generated using the OPLS3e force field, a default Van der Waals radius scaling factor of 1.0, and a charge cutoff of 0.25 [33].

5.4. Extra precision (XP) molecular docking simulation

Molecular docking simulation is an important key component for computer-aided drug design (CADD) approaches as well as structural biology-related research to predict bond geometry [37], binding affinities, and interactions between a receptor protein and ligand at the molecular level. The extra precision (XP) molecular docking between sleeted phytochemicals and Mpro was performed by the glide module in the Schrodinger suite [35]. The highest binding affinity of docked complexes was taken from the best poses and types of interactions of the ligand with the receptor molecules and illustrated by the Maestro Schrodinger visualizer [38].

5.5. Analyses of pharmacokinetics (PK), toxicity, and drug-able properties

The top four ligand molecules' pharmacokinetics (GI absorption and BBB permeant) and drug properties [physicochemical properties (MW, Heavy atoms, Aromatic heavy atoms, Rotatable bonds, H-bond acceptors and H-bond donors), Lipophilicity (Log Po/w(MLOGP), Water Solubility (Log S (ESOL)), Lipinski's rule of 5 (RO5) [39], and synthetic accessibility] were analyzed using the Swiss ADME (http://www.swissadme.ch/) server [40]. The toxicity (Carcinogenicity, Mutagenicity, Hepatotoxicity, Cytotoxicity and Rat oral acute toxicity) was predicted using a free web server, ProTox-II (https://tox-new.charite.de/) [41].

5.6. Molecular dynamic (MD) simulation

To determine the interaction rigidity and binding status of the receptor protein binding site cavity to the selected ligand molecules, the complex protein-ligand structure was evaluated with the distinct technology of MD simulation by creating an artificial biomolecular environment [42, 43]. A 100 ns MD simulation has been performed by the Desmond v3.6 Program in Schrodinger under the Linux (Ubuntu-20.04.1 LTS) operating system to identify the physical movements of the four highest binding score protein-ligand complexes [25].An examined three-site transferrable intermolecular potential (TIP3P) water model was implemented into the system, where an orthorhombic box shape with a 10 Å distance from the center has been used to sustain a specified volume. The whole system was neutralized by adding Na+ and Cl- with a salt concentration of 0.15 M and an OPLS3e force field was applied. Finally, the protein-ligand complex system was minimized with a natural time and pressure (NPT) ensemble, which was determined at constant pressure (101325 pascals) and 300 K temperature [44]. Furthermore, to assess the stability and dynamic characteristics of these complexes, root-mean-square deviation (RMSD), root mean square fluctuation (RMSF), radius of gyration (rGyr), and solvent accessible surface area (SASA) values were determined. The complete molecular docking and molecular dynamics simulations were run on a Linux (Ubuntu-20.04.1 LTS) machine with an Intel Core i7-10700K processor, 3200 MHz DDR4 RAM, and an RTX 3080 DDR6 8704 CUDA core GPU.

Acknowledgements: The authors are thankful to the management of P.R. Pote Patil College of Pharmacy for providing us with the facilities in order to carry out the research work.

Author contributions: Concept – V.R.M, M.G.T.; Design – V.R.M, M.G.T, P.J.B.; Supervision – M.G.T.; Resources – M.G.T, PJ.B., R.A.B; Materials – M.G.T, PJ.B., R.A.B.; Data Collection and/or Processing – V.R.M, M.G.T, P.J.B, CNV.; Analysis and/or Interpretation – V.R.M, M.G.T, P.J.B, CNV, VAB; Literature Search – PJ.B., R.A.B.; Writing – V.R.M., CNV, R.A.B, VAB; Critical Reviews – M.G.T, P.J.B

Conflict of interest statement: The authors declared no conflict of interest.

REFERENCES

[1] Peiris JS, Guan Y, Yuen K. Severe acute respiratory syndrome. Nat Med. 2004 Dec;10(12):S88-97. [CrossRef]

[2] Du L, He Y, Zhou Y, Liu S, Zheng BJ, Jiang S. The spike protein of SARS-CoV—a target for vaccine and therapeutic development. Nat Rev Microbiol. 2009 Mar;7(3):226-36. [CrossRef]

[3] Zaki AM, Van Boheemen S, Bestebroer TM, Osterhaus AD, Fouchier RA. Isolation of a novel coronavirus from a man with pneumonia in Saudi Arabia. New England Journal of Medicine. 2012 Nov 8;367(19):1814-20. [CrossRef]

[4] Wang C, Horby PW, Hayden FG, Gao GF. A novel coronavirus outbreak of global health concern. The lancet. 2020 Feb 15;395(10223):470-3. [CrossRef]

[5] Soni, A.K. Update on the SARS-CoV-2 (COVID-19) Outbreak: A Global Pandemic Challenge. Preprints 2020, 2020040082.[CrossRef]

[6] Zeidler A, Karpinski TM. SARS-CoV, MERS-CoV, SARS-CoV-2 comparison of three emerging Coronaviruses. Jundishapur Journal of Microbiology. 2020 Jun 30;13(6). [CrossRef]

[7] Synowiec A, Szczepański A, Barreto-Duran E, Lie LK, Pyrc K. Severe acute respiratory syndrome coronavirus 2 (SARS-CoV-2): a systemic infection. Clin Microbiol Rev. 2021 Apr 1;34(2):e00133-20. [CrossRef]

[8] De Giorgio A. Global Psychological Implications of Severe Acute Respiratory Syndrome Coronavirus 2 (SARS-CoV-2) and Coronavirus Disease-2019 (COVID-19). What Can Be Learned From Italy. Reflections, Perspectives, Opportunities. Frontiers in psychology.. 2020 Jul 24;11:1836.[CrossRef]

[9] van Dorp L, Acman M, Richard D, Shaw LP, Ford CE, Ormond L, Owen CJ, Pang J, Tan CC, Boshier FA, Ortiz AT. Emergence of genomic diversity and recurrent mutations in SARS-CoV-2. Infection, Genetics and Evolution. 2020 Sep 1;83:104351..[CrossRef]

[10] Shu Y, McCauley J. GISAID: Global initiative on sharing all influenza data–from vision to reality. Euro Surveill. 2017 Mar 30;22(13):30494. [CrossRef]

[11] Johansson MA, Quandelacy TM, Kada S, Prasad PV, Steele M, Brooks JT, Slayton RB, Biggerstaff M, Butler JC. SARS-CoV-2 transmission from people without COVID-19 symptoms. JAMA Netw Open. 2021 Jan 4;4(1):e2035057.[CrossRef]

[12] Oran DP, Topol EJ. The proportion of SARS-CoV-2 infections that are asymptomatic: a systematic review. Annals of internal medicine. 2021 May;174(5):655-62. [CrossRef]

[13] Tallei TE, Tumilaar SG, Niode NJ, Kepel BJ, Idroes R, Effendi Y, Sakib SA, Emran TB. Potential of plant bioactive compounds as SARS-CoV-2 main protease (Mpro) and spike (S) glycoprotein inhibitors: a molecular docking study. Scientifica. 2020 Dec 23;2020..[CrossRef]

[14] Alam R, Imon RR, Talukder ME, Akhter S, Hossain MA, Ahammad F, Rahman MM. GC-MS analysis of phytoconstituents from Ruellia prostrata and Senna tora and identification of potential anti-viral activity against SARS-CoV-2. RSC Adv. 2021;11(63):40120-35. [CrossRef]

[15] Dutta T, Paul A, Majumder M, Sultan RA, Emran TB. Pharmacological evidence for the use of Cissus assamica as a medicinal plant in the management of pain and pyrexia. Biochem Biophys Rep. 2020 Mar 1;21:100715.[CrossRef]

[16] Tareq AM, Farhad S, Uddin AN, Hoque M, Nasrin MS, Uddin MM, Hasan M, Sultana A, Munira MS, Lyzu C, Hossen SM. Chemical profiles, pharmacological properties, and in silico studies provide new insights on Cycas pectinata. Heliyon. 2020 Jun 1;6(6):e04061.[CrossRef]

[17] Banu N, Alam N, Nazmul Islam M, Islam S, Sakib SA, Hanif NB, Chowdhury MR, Tareq AM, Hasan Chowdhury K, Jahan S, Azad A. Insightful valorization of the biological activities of pani heloch leaves through experimental and computer-aided mechanisms. Molecules. 2020 Nov 5;25(21):5153. [CrossRef]

[18] Li W, Moore MJ, Vasilieva N, Sui J, Wong SK, Berne MA, Somasundaran M, Sullivan JL, Luzuriaga K, Greenough TC, Choe H. Angiotensin-converting enzyme 2 is a functional receptor for the SARS coronavirus. Nature. 2003 Nov;426(6965):450-4. [CrossRef]

[19] Hilgenfeld R. From SARS to MERS: crystallographic studies on coronaviral proteases enable antiviral drug design. FEBS J. 2014 Sep;281(18):4085-96. [CrossRef]

[20] Chen J, Malone B, Llewellyn E, Grasso M, Shelton PM, Olinares PD, Maruthi K, Eng ET, Vatandaslar H, Chait BT, Kapoor TM. Structural basis for helicase-polymerase coupling in the SARS-CoV-2 replication-transcription complex. Cell. 2020 Sep 17;182(6):1560-73. [CrossRef]

[21] Zhang L, Lin D, Sun X, Rox K, Hilgenfeld R. X-ray structure of main protease of the novel coronavirus SARS-CoV-2 enables design of α-ketoamide inhibitors. BioRxiv. 2020 Jan 1. [CrossRef]

[22] Yadav RP, Patel AK, Jagannadham MV. Neriifolin S, a dimeric serine protease from Euphorbia neriifolia Linn.: Purification and biochemical characterisation. Food chemistry. 2012 Jun 1;132(3):1296-304. [CrossRef]

[23] Yan SL, Li YH, Chen XQ, Liu D, Chen CH, Li RT. Diterpenes from the stem bark of Euphorbia neriifolia and their in vitro anti-HIV activity. Phytochemistry. 2018 Jan 1;145:40-7. [CrossRef]

[24] Li JC, Dai WF, Liu D, Jiang MY, Zhang ZJ, Chen XQ, Chen CH, Li RT, Li HM. Bioactive ent-isopimarane diterpenoids from Euphorbia neriifolia. Phytochemistry. 2020 Jul 1;175:112373. [CrossRef]

[25] Mali PY, Panchal SS. Euphorbia neriifolia L.: Review on botany, ethnomedicinal uses, phytochemistry and biological activities. Asian Pac J Trop Med. 2017 May 1;10(5):430-8. [CrossRef]

[26] Sarkar C, Mondal M, Torequl Islam M, Martorell M, Docea AO, Maroyi A, Sharifi-Rad J, Calina D. Potential therapeutic options for COVID-19: current status, challenges, and future perspectives. Front Pharmacol. 2020 Sep 15;11:572870. [CrossRef]

[27] Lordan R, Rando HM, Greene CS. Dietary supplements and nutraceuticals under investigation for COVID-19 prevention and treatment. Msystems. 2021 May 4;6(3):e00122-21. [CrossRef]

[28] Chang FR, Yen CT, Ei-Shazly M, Lin WH, Yen MH, Lin KH, Wu YC. Anti-human coronavirus (anti-HCoV) triterpenoids from the leaves of Euphorbia neriifolia. Nat Prod Commun 2012 Nov;7(11):1934578X1200701103. [CrossRef]

[29] Tai W, He L, Zhang X, Pu J, Voronin D, Jiang S, Zhou Y, Du L. Characterization of the receptor-binding domain (RBD) of 2019 novel coronavirus: implication for development of RBD protein as a viral attachment inhibitor and vaccine. Cell Mol Immunol. 2020 Jun;17(6):613-20.[CrossRef]

[30] Ahammad F, Alam R, Mahmud R, Akhter S, Talukder EK, Tonmoy AM, Fahim S, Al-Ghamdi K, Samad A, Qadri I. Pharmacoinformatics and molecular dynamics simulation-based phytochemical screening of neem plant (Azadiractha indica) against human cancer by targeting MCM7 protein. Brief Bioinform. 2021 Sep;22(5):bbab098. [CrossRef]

[31] Rose PW, Prlić A, Altunkaya A, Bi C, Bradley AR, Christie CH, Costanzo LD, Duarte JM, Dutta S, Feng Z, Green RK. The RCSB protein data bank: integrative view of protein, gene and 3D structural information. Nucleic acids research. 2016 Oct 27:gkw1000. [CrossRef]

[32] Madhavi Sastry G, Adzhigirey M, Day T, Annabhimoju R, Sherman W. Protein and ligand preparation: parameters, protocols, and influence on virtual screening enrichments. J Comput Aided Mol Des. 2013 Mar;27(3):221-34. [CrossRef]

[33] Harder E, Damm W, Maple J, Wu C, Reboul M, Xiang JY, Wang L, Lupyan D, Dahlgren MK, Knight JL, Kaus JW. OPLS3: a force field providing broad coverage of drug-like small molecules and proteins. J Chem Theory Comput. 2016 Jan 12;12(1):281-96. [CrossRef]

[34] Kim S, Thiessen PA, Bolton EE, Chen J, Fu G, Gindulyte A, Han L, He J, He S, Shoemaker BA, Wang J. PubChem substance and compound databases. Nucleic acids research. 2016 Jan 4;44(D1):D1202-13. [CrossRef]

[35] Bhachoo J, Beuming T. Investigating protein–peptide interactions using the Schrödinger computational suite. Modeling peptide-protein interactions. 2017:235-54. [CrossRef]

[36] Kalirajan R, Pandiselvi A, Gowramma B, Balachandran P. In-silico design, ADMET screening, MM-GBSA binding free energy of some novel isoxazole substituted 9-anilinoacridines as HER2 inhibitors targeting breast cancer. Current Drug Research Reviews Formerly: Curr Drug Abuse Rev. 2019 Dec 1;11(2):118-28. [CrossRef]

[37] Friesner RA, Murphy RB, Repasky MP, Frye LL, Greenwood JR, Halgren TA, Sanschagrin PC, Mainz DT. Extra precision glide: Docking and scoring incorporating a model of hydrophobic enclosure for protein− ligand complexes. J Med Chem. 2006 Oct 19;49(21):6177-96. [CrossRef]

[38] Hayes JM. An integrated visualization and basic molecular modeling laboratory for first-year undergraduate medicinal chemistry. J Chem Educ. 2014 Jun 10;91(6):919-23. [CrossRef]

[39] Giménez BG, Santos MS, Ferrarini M, Fernandes JP. Evaluation of blockbuster drugs under the rule-of-five. Die Pharmazie-An International Journal of Pharmaceutical Sciences. 2010 Feb 1;65(2):148-52. [CrossRef]

[40] Daina A, Michielin O, Zoete V. SwissADME: a free web tool to evaluate pharmacokinetics, drug-likeness and medicinal chemistry friendliness of small molecules. Sci Rep. 2017 Mar 3;7(1):1-3. [CrossRef]

[41] Banerjee P, Eckert AO, Schrey AK, Preissner R. ProTox-II: a webserver for the prediction of toxicity of chemicals. Nucleic acids research. 2018 Jul 2;46(W1):W257-63. [CrossRef]

[42] Cheatham III TE, Brooks BR. Recent advances in molecular dynamics simulation towards the realistic representation of biomolecules in solution. Theor Chem Acc. 1998 Sep;99(5):279-88. [CrossRef]

[43] Schlick T, Portillo-Ledesma S, Myers CG, Beljak L, Chen J, Dakhel S, Darling D, Ghosh S, Hall J, Jan M, Liang E. Biomolecular Modeling and Simulation: A Prospering Multidisciplinary Field. Annu Rev Biophys. 2021 Feb 19;50:267-301. [CrossRef]

[44] Roos K, Wu C, Damm W, Reboul M, Stevenson JM, Lu C, Dahlgren MK, Mondal S, Chen W, Wang L, Abel R. OPLS3e: Extending force field coverage for drug-like small molecules. J Chem Theory Comput. 2019 Feb 15;15(3):1863-74. [CrossRef]

[45] Zeidler A, Karpinski TM. SARS-CoV, MERS-CoV, SARS-CoV-2 comparison of three emerging Coronaviruses. Jundishapur Journal of Microbiology. 2020 Jun 30;13(6). [CrossRef]

[46] Karpiński TM, Ożarowski M, Seremak-Mrozikiewicz A, Wolski H, Wlodkowic D. The 2020 race towards SARS-CoV-2 specific vaccines. Theranostics. 2021;11(4):1690. [CrossRef]

[47] Kannan SR, Spratt AN, Sharma K, Chand HS, Byrareddy SN, Singh K. Omicron SARS-CoV-2 variant: Unique features and their impact on pre-existing antibodies. J Autoimmun. 2022 Jan 1;126:102779. [CrossRef]

[48] Rahimi F, Abadi AT. Is omicron the last SARS-CoV-2 variant of concern?. Arch Med Res. 2022 Apr 1;53(3):336-8. [CrossRef]

[49] Ghosh N, Nandi S, Saha I. A review on evolution of emerging SARS-CoV-2 variants based on spike glycoprotein. Int Immunopharmacol. 2022 Jan 29:108565. [CrossRef]

[50] Rahman SM, Atikullah M, Islam M, Mohaimenul M, Ahammad F, Saha B, Rahman M. Anti-inflammatory, antinociceptive and antidiarrhoeal activities of methanol and ethyl acetate extract of Hemigraphis alternata leaves in mice. Clinical phytoscience. 2019 Dec;5(1):1-3. [CrossRef]

[51] Mishra BB, Tiwari VK. Natural products: an evolving role in future drug discovery. Eur J Med Chem. 2011 Oct 1;46(10):4769-807. [CrossRef]

[52] ul Qamar MT, Alqahtani SM, Alamri MA, Chen LL. Structural basis of SARS-CoV-2 3CLpro and anti-COVID-19 drug discovery from medicinal plants. J Pharm Anal. 2020 Aug 1;10(4):313-9. [CrossRef]

[53] Anand U, Tudu CK, Nandy S, Sunita K, Tripathi V, Loake GJ, Dey A, Proćków J. Ethnodermatological use of medicinal plants in India: from ayurvedic formulations to clinical perspectives–a review. J Ethnopharmacol. 2022 Feb 10;284:114744. [CrossRef]

[54] Wan S, Bhati AP, Wade AD, Alfè D, Coveney PV. Thermodynamic and structural insights into the repurposing of drugs that bind to SARS-CoV-2 main protease. Mol Syst Des Eng. 2022;7(2):123-31. [CrossRef]

[55] Lordan R, Rando HM, Greene CS. Dietary supplements and nutraceuticals under investigation for COVID-19 prevention and treatment. Msystems. 2021 May 4;6(3):e00122-21. [CrossRef]

[56] Chang FR, Yen CT, Ei-Shazly M, Lin WH, Yen MH, Lin KH, Wu YC. Anti-human coronavirus (anti-HCoV) triterpenoids from the leaves of Euphorbia neriifolia. Nat Prod Commun. 2012 Nov;7(11):1934578X1200701103. [CrossRef]

[57] Upadhyaya C, Sathish S. A review on Euphorbia neriifolia plant. International Journal of Pharmaceutical Chemistry. 2017;3:149-54.

[58] Ahmed SA, Nazim S, Siraj S, Siddik PM, Wahid CA. Euphorbia neriifolia Linn: A phytopharmacological review. International research journal of pharmacy. 2011;2(5):41-8.

[59] Aljahdali MO, Molla MH, Ahammad F. Compounds identified from marine mangrove plant (Avicennia Alba) as potential antiviral drug candidates against WDSV, an in-silico approach. Marine drugs. 2021 Apr 28;19(5):253. [CrossRef]

[60] Hindle SJ, Munji RN, Dolghih E, Gaskins G, Orng S, Ishimoto H, Soung A, DeSalvo M, Kitamoto T, Keiser MJ, Jacobson MP. Evolutionarily conserved roles for blood-brain barrier xenobiotic transporters in endogenous steroid partitioning and behavior. Cell reports. 2017 Oct 31;21(5):1304-16. [CrossRef]

[61] Miller DS. Regulation of P-glycoprotein and other ABC drug transporters at the blood–brain barrier. Trends Pharmacol Sci. 2010 Jun 1;31(6):246-54. [CrossRef]

[62] Agúndez JA, Jiménez-Jiménez FJ, Alonso-Navarro H, García-Martín E. Drug and xenobiotic biotransformation in the blood–brain barrier: a neglected issue. Front Cell Neurosci. 2014 Oct 17;8:335. [CrossRef]

[63] Whitebread S, Hamon J, Bojanic D, Urban L. Keynote review: in vitro safety pharmacology profiling: an essential tool for successful drug development. Drug Discov Today. 2005 Nov 1;10(21):1421-33. [CrossRef]

[64] Ursu O, Rayan A, Goldblum A, Oprea TI. Understanding drug-likeness. Wiley Interdisciplinary Reviews: Computational Molecular Science. 2011 Sep;1(5):760-81. [CrossRef]

[65] Bade R, Chan HF, Reynisson J. Characteristics of known drug space. Natural products, their derivatives and synthetic drugs. Eur J Med Chem. 2010 Dec 1;45(12):5646-52. [CrossRef]

[66] Ertl P, Schuffenhauer A. Estimation of synthetic accessibility score of drug-like molecules based on molecular complexity and fragment contributions. J Cheminform. 2009 Dec;1(1):1-1. [CrossRef]

[67] Shree P, Mishra P, Selvaraj C, Singh SK, Chaube R, Garg N, Tripathi YB. Targeting COVID-19 (SARS-CoV-2) main protease through active phytochemicals of ayurvedic medicinal plants–Withania somnifera (Ashwagandha), Tinospora cordifolia (Giloy) and Ocimum sanctum (Tulsi)–a molecular docking study. J Biomol Struct Dyn. 2022 Jan 2;40(1):190-203. [CrossRef]

[68] Chaudhary M, Sehgal D. In silico identification of natural antiviral compounds as a potential inhibitor of chikungunya virus non-structural protein 3 macrodomain. J Biomol Struct Dyn. 2021 Jul 25:1-1. [CrossRef]

[69] RK M, AK N. In silico evaluation of multispecies toxicity of natural compounds. Drug and Chemical Toxicology. 2019 May 21;44(5):480-6. [CrossRef]

[70] Gadaleta D, Vuković K, Toma C, Lavado GJ, Karmaus AL, Mansouri K, Kleinstreuer NC, Benfenati E, Roncaglioni A. SAR and QSAR modeling of a large collection of LD50 rat acute oral toxicity data. J Cheminform. 2019 Dec;11(1):1-6. [CrossRef]

[71] Aljahdali MO, Molla MH, Ahammad F. Compounds identified from marine mangrove plant (Avicennia Alba) as potential antiviral drug candidates against WDSV, an in-silico approach. Marine drugs. 2021 Apr 28;19(5):253. [CrossRef]

[72] Ekins S, Freundlich JS. Validating new tuberculosis computational models with public whole cell screening aerobic activity datasets. Pharmaceutical research. 2011 Aug;28(8):1859-69. [CrossRef]

[73] Kaye J, Reeves R, Chaiten L. The mifepristone REMS: A needless and unlawful barrier to care☆. Contraception. 2021 Jul 1;104(1):12-5.[CrossRef]

[74] Liu X, Shi D, Zhou S, Liu H, Liu H, Yao X. Molecular dynamics simulations and novel drug discovery. Expert Opin Drug Discov. 2018 Jan 2;13(1):23-37. [CrossRef]

[75] Kalimuthu AK, Panneerselvam T, Pavadai P, Pandian SR, Sundar K, Murugesan S, Ammunje DN, Kumar S, Arunachalam S, Kunjiappan S. Pharmacoinformatics-based investigation of bioactive compounds of Rasam (South Indian recipe) against human cancer. Scientific reports. 2021 Nov 2;11(1):1-9. [CrossRef]

[76] Samad A, Huq M, Rahman M. Bioinformatics approaches identified dasatinib and bortezomib inhibit the activity of MCM7 protein as a potential treatment against human cancer. Scientific reports. 2022 Jan 27;12(1):1-6. [CrossRef]

[77] Sahoo S, Zhao X, Kyprianidis K. A review of concepts, benefits, and challenges for future electrical propulsion-based aircraft. Aerospace. 2020 Apr;7(4):44. [CrossRef]

[78] Sultan MT, Buttxs MS, Qayyum MM, Suleria HA. Immunity: plants as effective mediators. Crit Rev Food Sci Nutr. 2014 Jan 1;54(10):1298-308. [CrossRef]

[79] Atre NM, Khedkar DD. A Review on Herbal Remedies for Sexually Transmitted Infections (STIs) from Melghat Region of Maharashtra State, India. Eur. J. Med. Plants. 2020:1-7. [CrossRef]